

Laser Raman Temperature-Jump Study of the Kinetics of the Triiodide Equilibrium. Relaxation Times in the 10^{-8} – 10^{-7} Second Range^{1,2}

Douglas H. Turner,³ George W. Flynn,^{*4} Norman Sutin,^{*} and James V. Beitz

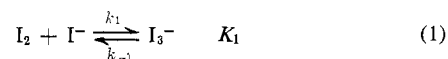
Contribution from the Departments of Chemistry, Brookhaven National Laboratory, Upton, New York 11973, and Columbia University, New York, New York 10027. Received July 9, 1971

Abstract: A laser temperature-jump apparatus for the study of chemical reactions with relaxation times in the 10^{-8} – 10^{-7} sec range is described. This apparatus makes use of the stimulated Raman effect in liquid nitrogen to shift the wavelength of the neodymium–glass laser radiation from 1.06 μ , where the absorbance of water is very small, to 1.41 μ , where water absorbs very strongly. The forward (k_1) and reverse (k_{-1}) rate constants for the reaction $I_2 + I^- \rightleftharpoons I_3^-$ have been measured by this technique; the values of k_1 and k_{-1} are $(6.2 \pm 0.8) \times 10^9 M^{-1} \text{sec}^{-1}$ and $(8.5 \pm 1.0) \times 10^6 \text{sec}^{-1}$, respectively, at 25° and 0.02 M ionic strength. Under the experimental conditions used the relaxation times of the system ranged from 30 to 70 nsec. The mechanism of the reaction is discussed.

Several attempts have been made in the past few years to develop a fast, sensitive, and convenient laser temperature-jump apparatus for the study of rapid chemical reactions in solution.^{5–9} The only commercially available lasers with enough power to produce useful temperature jumps are ruby and neodymium. These lasers operate at wavelengths of 0.694 and 1.06 μ , respectively. Since the absorbance of most solvents is negligible at 0.694 μ , use of a ruby laser requires that a suitable metal complex (usually a copper compound)⁶ or an organic dye (vanadyl phthalocyanine, for example)⁷ be added to the solution to absorb the laser radiation. Most solvents have higher absorbances in the near-infrared than in the visible region of the spectrum; however, the absorbance of water at 1.06 μ is still only 0.067 cm^{-1} . Evidently only a small fraction of the neodymium radiation is absorbed per unit path length of water and as a consequence not very large temperature jumps can be produced in water by the direct absorption of neodymium radiation; the largest temperature jump that has so far been produced in water by the direct absorption of Q-switched neodymium radiation is only a few tenths of a degree.³

Earlier we reported the successful heating of water by use of a Raman-shifted neodymium laser.¹⁰ The laser was operated in the Q-switched mode and liquid nitrogen was used to shift the wavelength of the neodymium radiation from 1.06 to 1.41 μ . The large ab-

sorbance of water at 1.41 μ leads to almost complete absorption of the stimulated Raman radiation. As a consequence, temperature jumps of a few degrees can readily be produced. We now wish to report the results of a study in which we have used this technique to measure the rate of formation of triiodide ions from iodine and iodide ions (reaction 1). Although this



reaction is too rapid for study by conventional temperature-jump techniques,¹¹ it has been studied by an nmr method.¹² In this method measurements were made of the effect of added iodine on the width of the ¹²⁷I nmr absorption line of the iodide ion in concentrated potassium iodide solutions. These experiments yielded a value of $(5.4 \pm 0.4) \times 10^{10} M^{-1} \text{sec}^{-1}$ for the rate constant for the formation of the triiodide ion at 35°. It has been pointed out, however, that this value of the rate constant is higher than a reasonable estimate of the diffusion-controlled limit.¹¹ In view of this disagreement, and because of our interest in this system, we decided to investigate the kinetics of the formation of triiodide ion by the laser temperature-jump method.

The thermodynamics of the formation of triiodide ion have been firmly established; the values of K_1 , ΔH_1 , and ΔS_1 , are 721 M^{-1} , $-4.76 \text{ kcal mol}^{-1}$, and $-2.88 \text{ cal deg}^{-1} \text{ mol}^{-1}$, respectively, at 25.0° and low ionic strength.^{13–15} These values do not change significantly when the solvent is changed from water to deuterium oxide,¹⁵ and K_1 does not vary appreciably with ionic strength, at least for potassium iodide concentrations up to 0.07 M and perchloric acid concentrations below 1.0 M .^{15,16}

Experimental Section

Apparatus. A schematic diagram of the apparatus used in this study is shown in Figure 1. The laser system consists of a neo-

(1) Research performed at Brookhaven National Laboratory under the auspices of the U. S. Atomic Energy Commission.

(2) Research supported in part by the National Science Foundation under Grant NSF-GP-10815 to Columbia University.

(3) National Institutes of Health Predoctoral Fellow, Fellowship, No. 5-F01-GM-41996-03, Columbia University, and Technical Collaborator, Brookhaven National Laboratory.

(4) Alfred P. Sloan Fellow and Research Collaborator, Brookhaven National Laboratory.

(5) H. Hoffmann, E. Yeager, and J. Stuehr, *Rev. Sci. Instrum.*, **39**, 649 (1968).

(6) H. Staerk and G. Czerninski, *Nature (London)*, **205**, 63 (1965); **207**, 399 (1965).

(7) E. F. Caldin, J. E. Crooks, and B. H. Robinson, *J. Sci. Instrum.*, **4**, 165 (1971).

(8) E. M. Eyring and B. C. Bennion, *Annu. Rev. Phys. Chem.*, **18**, 129 (1967).

(9) E. M. Eyring, Final Technical Report, AFOSR, Grant AF-AFOSR-476-66-A, Dec 1967.

(10) J. V. Beitz, G. W. Flynn, D. H. Turner, and N. Sutin, *J. Amer. Chem. Soc.*, **92**, 4130 (1970).

(11) M. Eigen and K. Kustin, *ibid.*, **84**, 1355 (1962).

(12) O. E. Myers, *J. Chem. Phys.*, **28**, 1027 (1958).

(13) A. D. Awtrey and R. E. Connick, *J. Amer. Chem. Soc.*, **73**, 1842 (1951).

(14) G. Daniele, *Gazz. Chim. Ital.*, **90**, 1078 (1960).

(15) R. W. Ramette and R. W. Sandford, *J. Amer. Chem. Soc.*, **87**, 5001 (1965).

(16) L. I. Katzin and E. Gebert, *ibid.*, **77**, 5814 (1955).

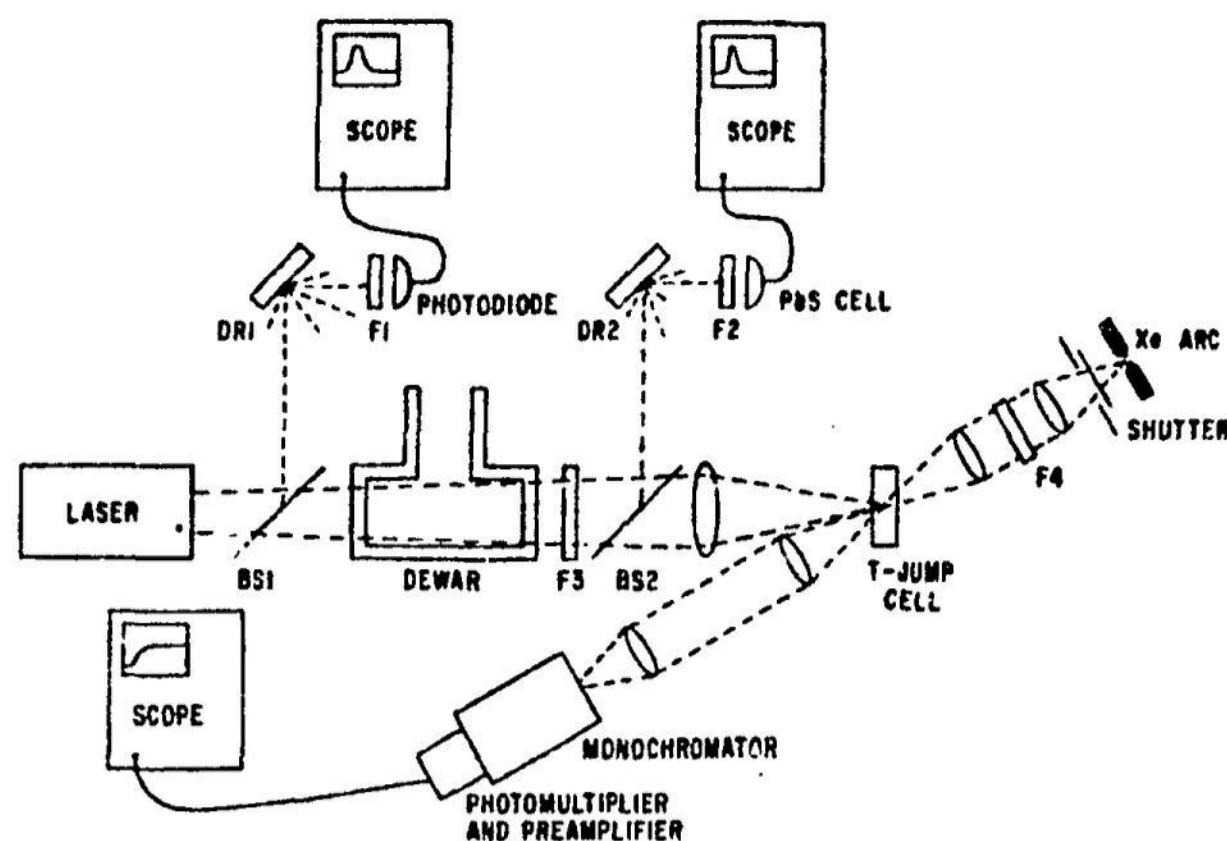


Figure 1. Schematic diagram of the laser Raman temperature-jump apparatus: BS1 and BS2 are beam splitters and DR1 and DR2 are diffuse reflectors; filters F1 and F2 transmit 1.06 and 1.41 μ , respectively, filter F3 is an Eastman dye solution (No. 9850) transmitting 1.41 μ but not 1.06 μ , and filter F4 transmits 0.353 μ .

dymium-glass, oscillator-amplifier combination with a Pockels cell Q switch. This system delivers a maximum energy of 20 J in 25 nsec at a wavelength of 1.06 μ . Beam divergence is controlled by a lens system between the oscillator and amplifier rods. The liquid nitrogen cell is a 20-cm long dewar fitted with 5-cm diameter, optical-quality quartz windows. Boiling of the liquid nitrogen along the optical path length was prevented by bubbling a gentle stream of helium through the liquid. The filter following the liquid nitrogen cell consists of a 1-cm long cell containing a solution of Kodak 9860 Q-switch dye in chlorobenzene. This solution very efficiently absorbs the 1.06- μ radiation which is not converted to 1.41 or 2.09 μ by the stimulated Raman process in the liquid nitrogen. The Raman radiation (which is not absorbed by the filter) is focused onto the sample cell by a quartz lens which is antireflection coated for 1.41 μ . The focused Raman radiation of 1-cm² cross-sectional area enters the sample cell almost normal to its front window. The sample cell is formed by two optical-quality quartz plates with an 0.8-mm thick Teflon spacer between them. This cell is mounted on a metal block in a Lucite housing and its temperature is controlled by circulating water from a constant temperature bath through the metal block.

A light beam from a 450-W Xenon lamp is used to monitor the reactions in the cell. This probe beam is focused in the middle of the sample cell so that the Raman radiation and the light from the Xenon lamp overlap spatially in the cell (the angle between the directions of the two beams is about 15°). A remote-controlled shutter is placed between the Xenon lamp and the sample cell. After passing through the sample cell the probe beam is reflected and refocused into a 0.25-meter monochromator. In the present experiments this monochromator was set at 0.353 μ , and a filter transmitting this wavelength was placed between the Xenon lamp and the sample cell. The monochromator is followed by a photomultiplier (RCA 1P 28)¹⁷ and preamplifier having a combined band width in excess of 30 MHz. Signals from the preamplifier are displayed and photographed on a Tektronix 7704 oscilloscope with a 100-MHz bandwidth.

Laser energy at 1.06 μ and Raman energy at 1.41 μ were measured by placing a ballistic thermopile after beam splitters 1 and 2, respectively, in Figure 1. Pulse widths at 1.06 μ were determined with an 0.1-nsec risetime photodiode while pulse widths at 1.41 μ were determined using an InAs detector having a rise time faster than 1 nsec. The output of both detectors was displayed on the same oscilloscope used for the T-jump measurements.

During a T-jump experiment a small fraction (<5%) of the 1.06- μ radiation is taken out of the laser beam by the beam splitter in front of the liquid nitrogen dewar and fed to the 1.06- μ photodiode. In a similar way the beam splitter following the filter which removed 1.06- μ radiation serves to deflect Raman radiation to a 1.41- μ detector. This allows the laser and Raman energies to be monitored for each laser pulse. Both detectors were calibrated with the ballistic thermopile.

(17) J. W. Hunt and J. K. Thomas, *Radiat. Res.*, **32**, 149 (1967). A 1000-ohm (instead of 50 ohm) resistor was used to terminate dynode 6 of the photomultiplier in our studies.

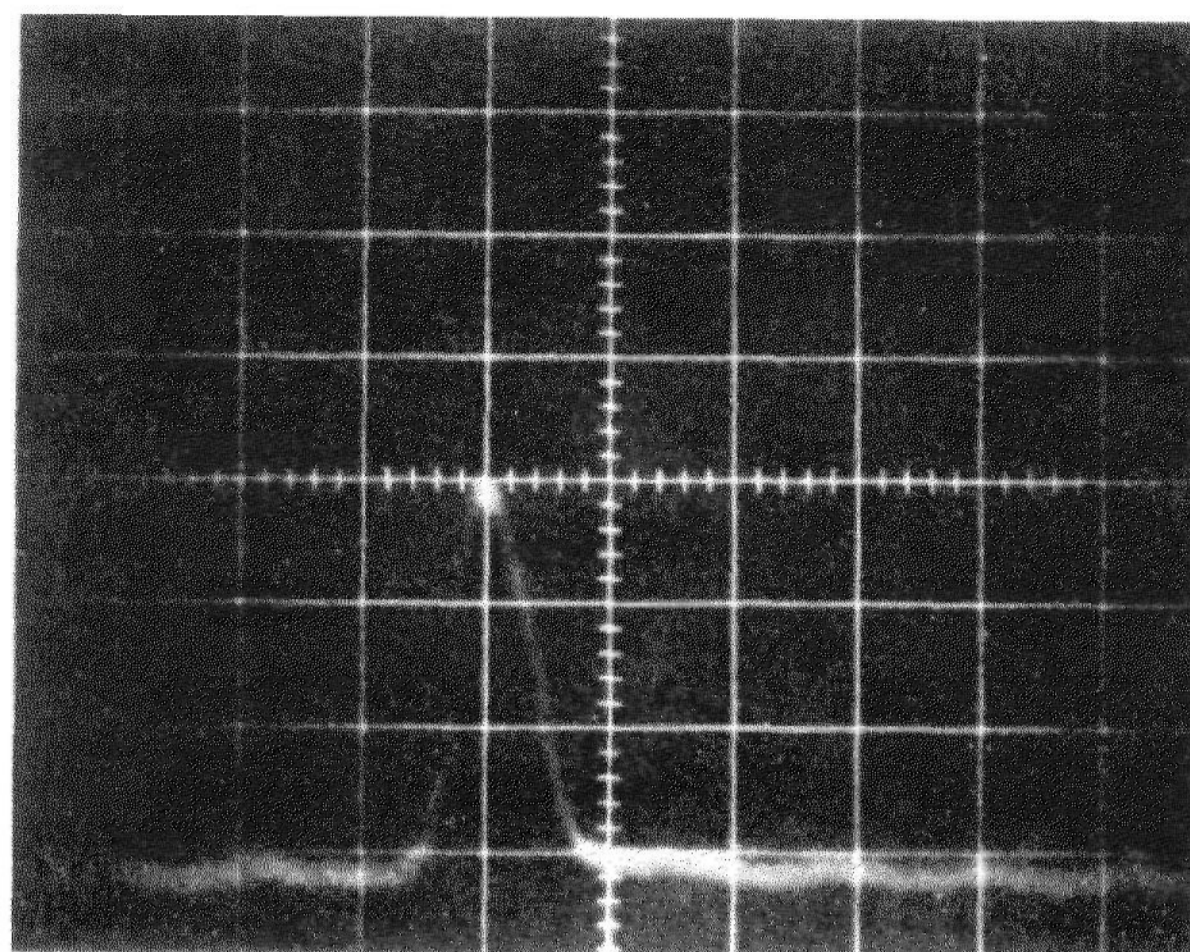


Figure 2. Oscilloscope photograph of the 1.41- μ stimulated Raman pulse: horizontal scale is 20 nsec per major division.

Procedure. Solutions containing 0.01 M perchloric acid, varying amounts of potassium iodide and iodine, and sufficient potassium perchlorate to adjust the ionic strength to 0.02 M were prepared in 50% H₂O-D₂O mixtures. The latter medium was chosen for the T-jump measurements because of the very large absorbance (10 cm⁻¹) of H₂O at 1.41 μ . The absorbance of D₂O is only 0.07 cm⁻¹ at this wavelength and consequently the temperature gradient produced in the solution by the T jump is lower in H₂O-D₂O mixtures than in pure H₂O.¹⁰ As mentioned above, the thermodynamic parameters for the triiodide equilibrium are identical in H₂O and D₂O, within the experimental error of the measurements.¹⁶ The compositions of the solutions prepared for the T-jump measurements were checked by measuring their absorbances at 0.353 μ , which is an absorbance maximum of the triiodide ion. The measured absorbances were in good agreement with the calculated values. For the T-jump measurements, portions of the solutions were placed in the sample cell and allowed to thermally equilibrate for at least 10 min. The shutter between the xenon lamp and the sample cell was then opened, the laser was fired, and the shift of the equilibrium produced by the T jump was followed by monitoring the absorbance changes at 0.353 μ . The oscilloscope traces were photographed and the energies of the laser pulse at 1.06 μ and of the Raman radiation at 1.41 μ were recorded. Each solution was T jumped at least four times, some as often as 12 times, and the relaxation times were calculated from the photographs of the oscilloscope traces.

Results

Raman Pulse Width and Energy. An oscilloscope photograph of the 1.41- μ stimulated Raman pulse is shown in Figure 2. The full width at half maximum height is 14–18 nsec which is slightly less than the 20–25-nsec width observed for the 1.06- μ laser pulse. The Raman pulse width determines the fastest reaction rate which can be studied with the present apparatus since the vibrational relaxation time of water is not expected to be a limiting factor. The energy of the 1.41- μ stimulated Raman pulse determined with the ballistic thermopile was usually about 2 J and varied by less than 10% over a series of measurements. The rate of heating of the sample can be determined if the total energy delivered to the sample in a given time is known. The integrated energy of a typical 1.41- μ Raman pulse as a function of time is shown in Figure 3. As can be seen, about 90% of the Raman pulse energy is delivered to the sample in about 25 nsec.

Uniformity of Heating and Acoustic Effects. The absorption of radiation by a medium leads to an increase in its temperature. This temperature increase can be

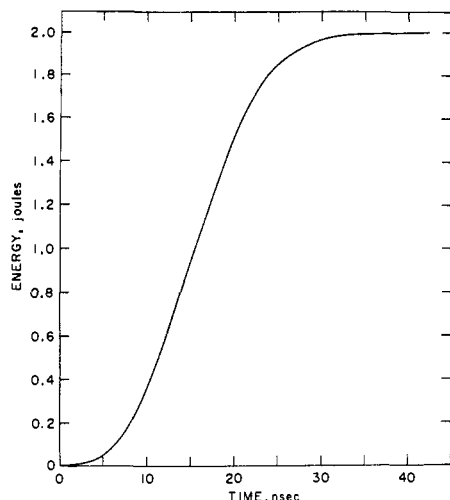


Figure 3. Plot of integrated energy as a function of time for a typical 1.41- μ stimulated Raman pulse.

calculated if the absorption profile of the medium and the energy density of the incident radiation are known. Since the vibration-translation relaxation time for liquid water is much less than the width of the Raman pulse, saturation of the absorption at 1.41 μ is not expected to occur. In such a situation the intensity of the radiation, $I(x)$, at a distance x cm from the front surface of the medium, is related to I_0 , the incident intensity (in cal cm^{-2}) by the Lambert expression

$$I(x) = I_0 \exp(-2.303Ax) \quad (2a)$$

where A is the absorbance of the medium per centimeter. Consequently, the temperature increase at a distance x , $\Delta T(x)$, is related to ΔT_0 , the temperature increase at the front surface of the medium, by the expression

$$\Delta T(x) = \Delta T_0 \exp(-2.303Ax) \quad (2b)$$

The value of ΔT_0 may be estimated as follows. When $2.303Ax \ll 1$, then eq 2a may be expanded to give

$$dI_0 = I_0 2.303A dx \quad (2c)$$

Since $\Delta T_0 = dI_0/C dx$, where C is the heat capacity of the medium in cal $\text{cm}^{-3} \text{deg}^{-1}$, it follows that

$$\Delta T_0 = 2.303AI_0/C \quad (2d)$$

Another useful parameter is the average temperature rise, $\overline{\Delta T}$, defined by

$$\overline{\Delta T} = 1/L \int_0^L \Delta T(x) dx \quad (3a)$$

where L is the length of the sample cell. Substituting the expression for $\Delta T(x)$ in eq 3a and integrating gives the equation

$$\overline{\Delta T} = (I_0/CL)[1 - \exp(-2.303AL)] \quad (3b)$$

In the present experiments, $I_0 = 0.5 \text{ cal/cm}^2$, $C = 1 \text{ cal cm}^{-3} \text{deg}^{-1}$, $L = 0.08 \text{ cm}$, and $A = 10$ and 4.3 cm^{-1} for H_2O and 50% $\text{H}_2\text{O}-\text{D}_2\text{O}$, respectively, at 1.41 μ . Substitution in eq 2 and 3 gives $\Delta T_0 = 11^\circ$, $\overline{\Delta T} = 5^\circ$ for H_2O and $\Delta T_0 = 4.7^\circ$, $\overline{\Delta T} = 3.4^\circ$ for 50% $\text{H}_2\text{O}-\text{D}_2\text{O}$. Since the laser oscillates in many high-order

transverse modes, the radiation intensity is nearly constant over the cross-sectional area of the Raman beam. The major source of temperature inhomogeneity is thus due to the exponential absorption noted above.

The temperature increase in the sample resulting from the absorption of the radiation occurs essentially at constant volume and produces as a consequence a relatively large increase in pressure. The pressure increase produced by the temperature jump may be estimated as follows. Since $V = f(P, T)$ it follows that

$$dV = \left(\frac{\partial V}{\partial T}\right)_P dT + \left(\frac{\partial V}{\partial P}\right)_T dP \quad (4)$$

For a process at constant volume, $dV = 0$, and therefore

$$\left(\frac{\partial P}{\partial T}\right)_V = -\left(\frac{\partial V}{\partial T}\right)_P / \left(\frac{\partial V}{\partial P}\right)_T = \alpha/\beta \quad (5)$$

where α is the coefficient of isobaric expansion and β is the isothermal compressibility of the medium. For H_2O at 20° , $\alpha = 2.0 \times 10^{-4} \text{ deg}^{-1}$ and $\beta = 45.3 \times 10^{-6} \text{ atm}^{-1}$; consequently $(\partial P/\partial T)_V = 4.4 \text{ atm deg}^{-1}$ at this temperature. The pressure increase accompanying a temperature jump in H_2O at room temperature is evidently quite large. This pressure increase will move through the medium as an acoustic wave and will give rise to a change in the temperature of the medium. This temperature change, which occurs adiabatically in an ideal fluid when viscosity and thermal conductivity effects can be neglected, is given by¹⁸

$$(\partial T/\partial P)_S = TV\alpha/C_p \quad (6)$$

where V is the molar volume and C_p is the molar heat capacity of the medium. For H_2O at 20° , $\Delta T = 0.03^\circ$ when $\Delta P = 20 \text{ atm}$. In the present experiments thermal conduction does occur so that the solution is not an ideal fluid; however, the heat conduction is so slow that it may be neglected over times of the order of milliseconds after heating. Thus the liquid may be assumed to be ideal, and the temperature rise due to sound propagation remains very small. Detailed treatments of this problem are available elsewhere.^{19,20}

In order to avoid complications such as cavitation and refractive index changes which are associated with the acoustic wave, temperature jumps in H_2O systems are usually made near 4° , where α , and therefore also $(\partial P/\partial T)_V$ and $(\partial T/\partial P)_S$, are zero.²¹ However, since the acoustic wave moves with the speed of sound it normally takes a few microseconds for cavitation effects to develop. As a consequence, relaxations which are sufficiently fast will be complete before the onset of cavitation. This is shown in Figure 4 in which an oscilloscope photograph of the absorbance change at 0.353 μ following a temperature jump at room temperature is reproduced on a long-time scale. As can be seen, the relaxation of the triiodide system is complete well before cavitation occurs.

Bandwidth and Risetime Considerations. The finite bandwidth of the amplifier and the finite width of the

(18) L. D. Landau and E. M. Lifshitz, "Fluid Mechanics," Addison-Wesley, Reading, Mass., 1959, Chapter 1, p 4; Chapter 8, p 247.

(19) P. R. Longaker and M. M. Litvak, *J. Appl. Phys.*, **10**, 4033 (1969).

(20) R. D. Bates Jr., G. W. Flynn, J. T. Knudtson, and A. M. Ronn, *J. Chem. Phys.*, **53**, 3621 (1970).

(21) M. Eigen and L. de Maeyer in "Technique of Organic Chemistry," Vol. VIII, Part II, A. Weissberger, Ed., Interscience, New York, N. Y., 1963, Chapter 18, p 973.

heating pulse could affect the signals observed in the present experiments. An estimate of the importance of these two factors can be made as follows.

1. Electronic Bandwidth. The absolute value of the gain of a typical amplifier as a function of frequency ω in the high frequency range is

$$|G(\omega)| \sim 1/[1 + \omega^2\tau_1^2]^{1/2} \quad (7)$$

The response time of the amplifier, τ_1 , can be determined if the bandwidth of the amplifier is known. In the present experiments $\tau_1 \simeq 9$ nsec ($\Delta\nu = 30$ MHz). The effect of this bandwidth on the signal risetime can be calculated by assuming that the heating pulse is instantaneous. Under these conditions the time-dependent input signal $f(t)$ is a single exponential (in the present experiments). In other words

$$f(t) \sim 1 - e^{-t/\tau_2}, t \geq 0 \quad (8)$$

where τ_2 is the true risetime of the signal. The absolute value of the Fourier transform of the time-dependent part of $f(t)$ is

$$|F(\omega)| \sim 1/[1 + \omega^2\tau_2^2]^{1/2} \quad (9)$$

For an input $F(\omega)$ to an amplifier of gain $G(\omega)$ the resulting output in the frequency domain is

$$|H(\omega)| \sim |F(\omega)||G(\omega)| \quad (10)$$

Under the conditions used in the present experiments, an excellent approximation for the amplifier output is

$$|H(\omega)| \sim 1/\sqrt{1 + \omega^2(\tau_1^2 + \tau_2^2)} \quad (11)$$

In the time domain this output has the appearance of an exponential e^{-t/τ_3} with $\tau_3^2 = \tau_1^2 + \tau_2^2$. The imaginary parts of the Fourier transforms lead to a frequency-dependent phase shift which is sufficiently small that the relation $\tau_3^2 = \tau_1^2 + \tau_2^2$ is still a good approximation for the observed signals.²² Thus the signal output has the form $1 - e^{-t/\tau_3}$. The minimum τ_3 observed in this work is 30 nsec giving $\tau_2 \simeq 28.6$ nsec for $\tau_1 = 9$ nsec. This corresponds to an error of the order of 5% for the *fastest* rates measured.

2. Heating Pulse Width. The electronic limitations considered above do not take into account the finite width of the heating pulse. If τ_2 is the exponential risetime measured with an infinite electronic bandwidth but for a finite heating pulse, then $\tau_2 > \tau_s$ where τ_s is the risetime measured for a heating pulse which is instantaneous. The finite width of the Raman pulse contributes directly to τ_s and not to the electronic risetime. In the case of an exponential signal $f(t)$ which, by definition, obeys the differential equation

$$d[f(t)]/dt + f(t)/\tau_s = 0 \quad (12)$$

where τ_s is a constant, the effect of a finite heating time can be determined very simply. If the heating-pulse stepfunction is $g(t)$, the differential equation for $f(t)$ becomes

$$d[f(t)]/dt + f(t)/\tau_s = g(t) \quad (13)$$

For times greater than 25 nsec (see Figure 3) $g(t)$ becomes a constant. The solution to eq 13 when $g(t)$

(22) D. M. Hunten, "Introduction to Electronics," Holt, Rinehart and Winston, New York, N. Y., 1964, p 102; G. E. Valley and H. Wallman, "Vacuum Tube Amplifiers," McGraw-Hill, New York, N. Y., 1948.

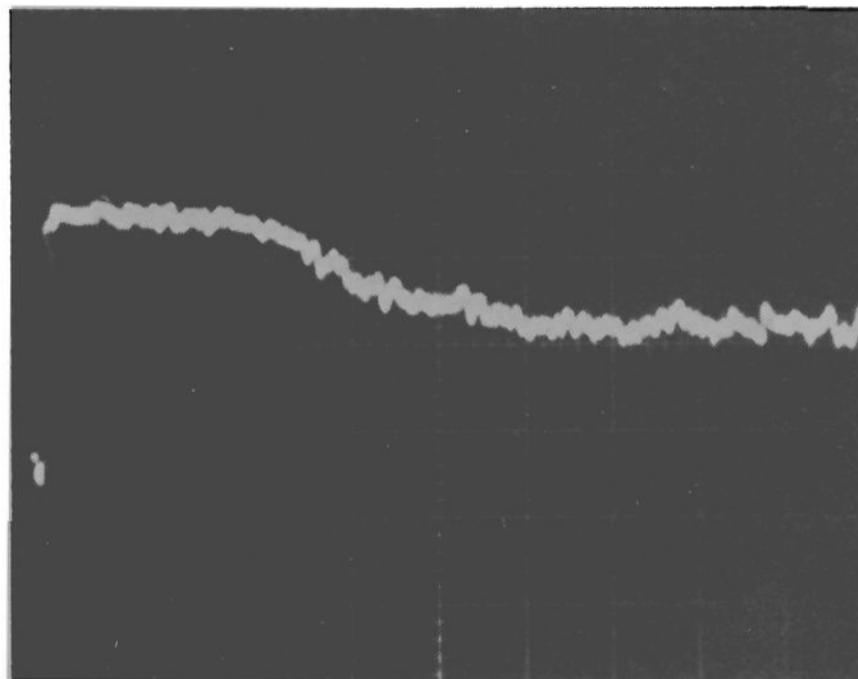


Figure 4. Oscilloscope photograph of the absorbance change at 0.353μ in the triiodide system following a temperature jump at room temperature: horizontal scale is 1μ sec per major division.

is a constant is an exponential with relaxation time τ_s . In all kinetic runs the data were analyzed only in the region where $g(t)$ was constant. Thus the experimental rates measured were limited only by the electronic response of the system. This introduces less than 5% error for the fastest rates as noted above.

Kinetic Measurements. Typical temperature-jump relaxation spectra are shown in Figure 5. These relaxation spectra are characterized by relaxation times τ defined by eq 14 where $(I_3^-)_{eq}$ is the concentration of

$$\frac{d(I_3^-)}{dt} = \frac{1}{\tau}[(I_3^-)_{eq} - (I_3^-)] \quad (14)$$

the triiodide ion at equilibrium. Values of the relaxation time were determined from the slopes of plots of $\log(I_\infty - I)$ vs. time (since the change in the light intensity is directly proportional to the change in the triiodide concentration) and, in some instances, also by the Guggenheim method. These relaxation times together with the equilibrium concentration of the iodide ion and iodine are presented in Table I. The slower reactions gave good kinetic plots. The kinetic plots for the faster reactions were somewhat curved initially (see bottom curve of Figure 5), presumably because the heating time is not "instantaneous" compared to the fastest relaxation times (Figure 3). In the latter cases the relaxation times were calculated from the linear portions of the $\log(I_\infty - I)$ vs. time plots.

Several observations provide strong evidence that two-photon processes are not responsible for the relaxations. The amplitudes of the signals were found to depend linearly on the Raman power. Moreover, the time required for the absorbance to return to its initial value was approximately 1 sec indicating that excited states are not involved. Finally, no relaxations were observed in iodine solutions in the absence of added iodide ions.

It can readily be shown that the relaxation times are related to the rate constants k_1 and k_{-1} and the equilibrium concentrations of iodine and iodide ion by eq 15.

$$\frac{1}{\tau} = k_{-1} + k_1[(I_2)_{eq} + (I^-)_{eq}] \quad (15)$$

The plot suggested by eq 15 is shown in Figure 6. Evi-

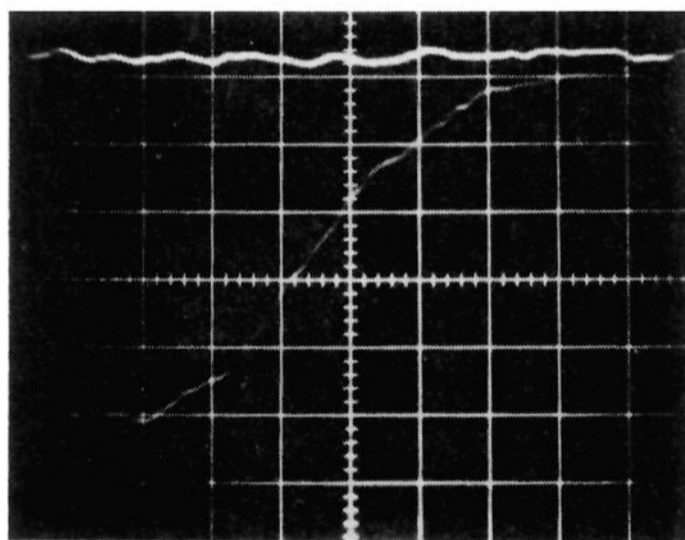
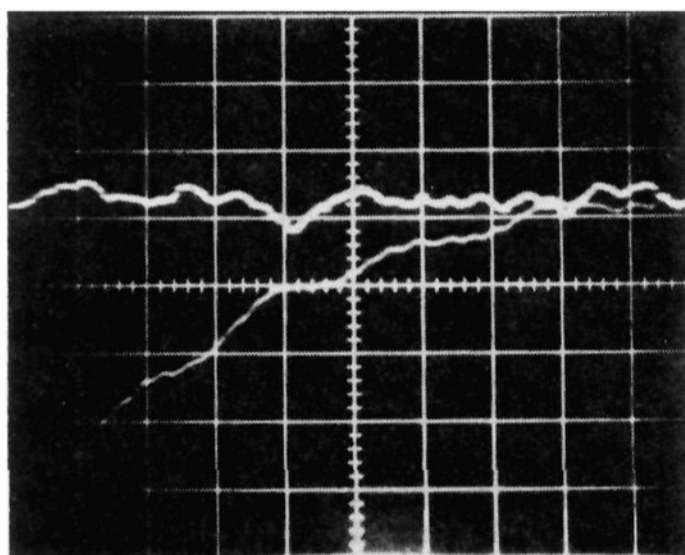
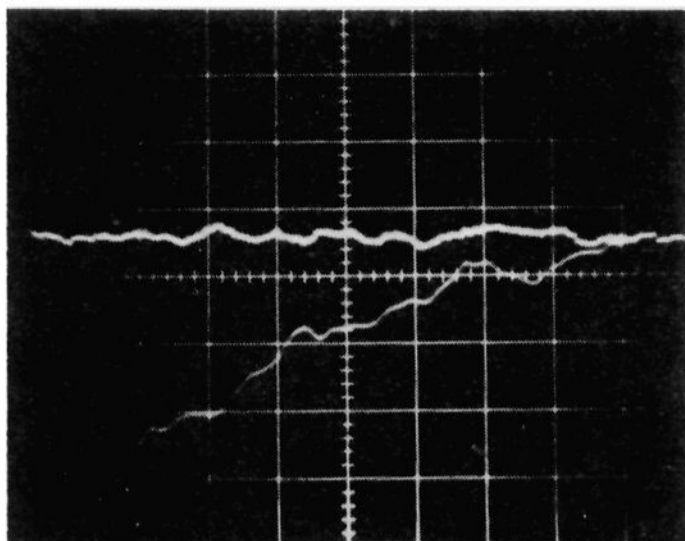


Figure 5. Temperature-jump relaxation spectra: horizontal scale is 20 nsec per major division, vertical scale is 50 mV per major division. Upper curve: $(I^-)_{eq} = 0.57 \times 10^{-3} M$, $(I_2)_{eq} = 0.36 \times 10^{-3} M$, $\tau = 67$ nsec. Middle curve: $(I^-)_{eq} = 1.58 \times 10^{-3} M$, $(I_2)_{eq} = 0.24 \times 10^{-3} M$, $\tau = 51$ nsec. Lower curve: $(I^-)_{eq} = 2.39 \times 10^{-3} M$, $(I_2)_{eq} = 0.39 \times 10^{-3} M$, $\tau = 34$ nsec. The vertical scale is a direct measure of the transmitted light intensity. The second "infinity" sweeps (100 nsec per major division) were triggered 1.2 μ sec after the initiation of the first sweep.

dently the kinetic data satisfy eq 15 reasonably well. The values of k_1 and k_{-1} calculated from the slope and intercept of this plot are $(6.2 \pm 0.8) \times 10^9 M^{-1} \text{sec}^{-1}$ and $(8.5 \pm 1.0) \times 10^6 \text{sec}^{-1}$, respectively, at 25°. Since $k_1/k_{-1} = K_1$, the value of the equilibrium constant for the reaction may be obtained from the rate measurements. These measurements give $K_1 = (7.3 \pm 1.3) \times$

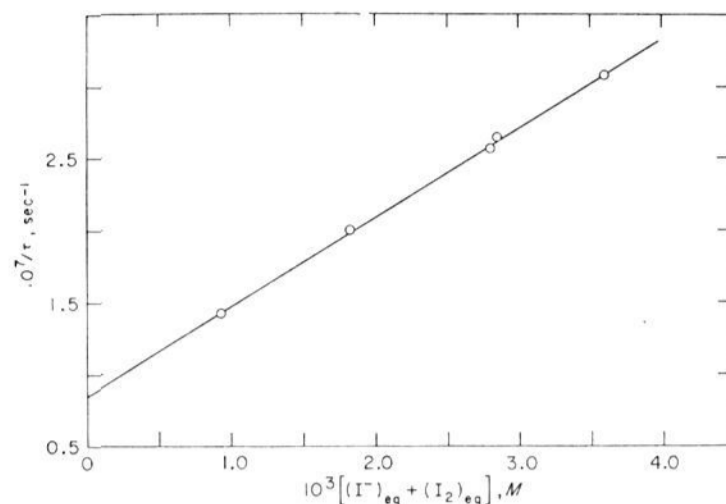


Figure 6. Plot of reciprocal relaxation time vs. $[(I^-)_{eq} + (I_2)_{eq}]$ at 25° and 0.02 M ionic strength.

$10^2 M^{-1}$, in excellent agreement with the value of K_1 determined directly.¹⁵

Discussion

The rate constant for the formation of triiodide ion determined in this work may be compared with the value calculated from simple diffusion theory. According to this theory,²³ the rate constant for a diffusion-controlled reaction (in which interionic forces may be neglected) is given by

$$k_{\text{diff}} = 4\pi N(r_1 + r_2)(D_1 + D_2)/1000 \quad (16)$$

where r_1 , r_2 , D_1 , and D_2 are the radii and diffusion coefficients, respectively, of the two reactants. Substitution of 2.16×10^{-8} and 2.52×10^{-8} cm for the radii, and 2.05×10^{-5} and 2.25×10^{-5} $\text{cm}^2 \text{sec}^{-1}$ for the diffusion coefficients of the iodide ion and iodine molecule,

Table I. Relaxation Times for the Triiodide System at 25°^a and 0.02 M Ionic Strength

$10^3(I^-)_{eq}$, M	$10^3(I_2)_{eq}$, M	τ , ^b nsec
0.57	0.36	70.7 ± 3.5
1.58	0.24	50.0 ± 5.2
2.39	0.39	39.0 ± 4.4
2.68	0.16	37.9 ± 4.4
3.45	0.14	32.4 ± 4.0

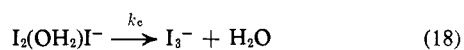
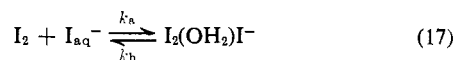
^a Temperature of the sample before the temperature jump plus 3.4°. ^b The quoted uncertainties are the standard deviations from the mean.

respectively, gives $k_{\text{diff}} = 1.5 \times 10^{10} M^{-1} \text{sec}^{-1}$ at 25°. This estimate of the rate constant for the diffusion-controlled reaction is a factor 2.5 times faster than the value of k_1 determined in this work suggesting that the reaction of iodine with iodide ion is, at least in part, activation controlled.²⁴

(23) M. V. Smoluchowski, *Z. Physik.*, **17**, 557, 583 (1916); *Z. Physik. Chem. (Leipzig)*, **92**, 129 (1917).

(24) Equation 16 assumes that the two reactants are spherically symmetrical. Since this is not the case in the system under study, it might be expected that a steric factor of the order of 2–4 should be introduced to correct for the absence of spherical symmetry. However, such a steric factor would be applied to the reaction rate for the reactants in contact and would have little effect on the magnitude of the diffusion-limited rate constant because the reactants make many (10–100) collisions for every encounter. In other words, the "steric factors" for diffusion-controlled reactions are much closer to unity than expected on the basis of purely geometrical considerations. Although there are, of course, other uncertainties in the application of eq 16 to the triiodide system, we feel that the disagreement between the observed and calculated rate constants is outside this uncertainty.

In common with complex-formation reactions of metal ions, the reaction of iodine with iodide ions may be assumed to proceed *via* the formation of an outer-sphere complex. This is illustrated in reactions 17 and 18. The iodine molecule and the iodide ion are



separated by a water molecule in the outer-sphere complex $\text{I}_2(\text{OH}_2)\text{I}^-$. In terms of this interpretation the first step in the reaction is the diffusion-controlled formation of the outer-sphere complex, and the second step is the formation of triiodide ion. The rate constant for the formation of the outer-sphere complex may be estimated from eq 16 with r_1 equal to $(2.05 + 2r_w) \times 10^{-8}$ cm where $2r_w$ is the diameter of a water molecule (2.76×10^{-8} cm). This procedure gives $k_a = 2.4 \times 10^{10} \text{ M}^{-1} \text{ sec}^{-1}$. The value of the outer-sphere association constant may be calculated from eq 19²⁵

$$K_0 = 4\pi N a^3 / 3(1000) \quad (19)$$

where a is the distance between the centers of the two reactants in the outer-sphere complex. Substitution of $a = (r_1 + r_2 + 2r_w)$ in eq 19 gives $K_0 = 1.0 \text{ M}^{-1}$. Finally, the steady-state approximation for the concentration of the outer-sphere complex leads to the following expression for the formation rate constant

(25) W. R. Gilkerson, *J. Chem. Phys.*, **25**, 1199 (1956); R. M. Fuoss, *J. Amer. Chem. Soc.*, **79**, 3301 (1957).

$$k_1 = k_a k_c / (k_b + k_c) \quad (20)$$

Substitution in eq 20, and remembering that $K_0 = k_a/k_b$, yields $k_c = 8 \times 10^9 \text{ sec}^{-1}$. The rate constant k_c provides an estimate of the lower limit of the rate constant for water exchange on the iodide ion.²⁶ The value of $\geq 8 \times 10^9 \text{ sec}^{-1}$ for this process seems reasonable since the rate constant for water exchange on cesium ion is $5 \times 10^9 \text{ sec}^{-1}$ ²⁷ and water exchange on this ion is almost certainly slower than water exchange on the larger, negatively charged, structure-breaking iodide ion.

The relaxation times measured in this work are almost two orders of magnitude faster than those previously measured by the temperature-jump method. As has been pointed out,¹⁰ it may be possible to obtain heating times of 10^{-8} sec or less by using a cavity-dumped or mode-locked laser. Another advantage of the laser temperature-jump technique is that it may readily be used with a variety of sample cells and reaction media. These and other aspects of the laser temperature-jump technique are currently being actively explored.

Acknowledgments. The authors wish to acknowledge helpful discussions with Dr. Harold Schwarz, Dr. James Muckerman, and Mr. Ronald Withnell. They also wish to thank Mr. Withnell for the design and construction of the preamplifier.

(26) Only a lower limit for the water exchange rate is estimated since it is possible for exchange of the relatively light water molecule in the outer-sphere complex to occur several times before the complex collapses to the triiodide ion.

(27) M. Eigen, *Proc. Int. Conf. Coord. Chem.*, **8th**, 67 (1963).

Thermodynamics of the Reversible Oxygenation of Amine Complexes of Cobalt(II) Protoporphyrin IX Dimethyl Ester in a Nonaqueous Medium

Helen C. Stynes and James A. Ibers*

Contribution from the Department of Chemistry, Northwestern University, Evanston, Illinois 60201. Received June 24, 1971

Abstract: The equilibrium constant for the reversible binding of molecular oxygen to cobalt(II) protoporphyrin IX dimethyl ester in a nonaqueous medium, a simple model system for oxygen-carrying hemoproteins, has been measured in the temperature range -31 to -63° . Pyridine, 4-*tert*-butylpyridine, and 1-methylimidazole were used as ligands in the fifth coordination site. The measurements were carried out using visible spectroscopy. The standard enthalpy changes for O_2 binding to cobalt protoporphyrin IX dimethyl ester are -9.2 ± 1.0 , -10.0 ± 0.5 , and -11.5 ± 1.0 kcal/mol when pyridine, 4-*tert*-butylpyridine, and 1-methylimidazole are the ligands in the fifth coordination site respectively. The standard entropy changes are -53 ± 5 , -57 ± 2 , and -58 ± 4 eu, respectively, with a 1-Torr standard state. These data may be compared with those in the literature of -18.1 kcal/mol and -60 eu for myoglobin. Possible reasons for the marked differences in standard enthalpy between the model cobalt system and myoglobin are discussed.

In the course of our attempts to isolate crystals of a molecular oxygen complex of a cobalt porphyrin, it became necessary to make a detailed investigation of the conditions under which these metal porphyrins bind oxygen reversibly. We wish to report the first data on the thermodynamics of the reversible binding of molecular oxygen to a cobalt porphyrin. These

measurements are further extensions of our studies on the binding of small molecules to transition metals and are of considerable biological interest as the metal porphyrin serves as a model system for the hemoproteins.

Although qualitative esr studies have been carried out on the ability of cobalt(II) porphyrins to carry